THE JOURNAL OF BIOLOGICAL CHEMISTRY
Vol. 273, No. 33, Issue of August 14, pp. 20960–20966, 1998

Printed in U.S.A.

Biochemical Characterization of WrbA, Founding Member of a New Family of Multimeric Flavodoxin-like Proteins*

(Received for publication, November 11, 1997, and in revised form, May 27, 1998)

Rita Grandori‡, Peter Khalifah, Judith A. Boice§¶, Robert Fairman§‖, Kira Giovanielli, and Jannette Carey‡‡**

From the Department of Chemistry, Princeton University, Princeton, New Jersey 08544-1009 and the §Bristol-Myers Squibb Pharmaceutical Research Institute, Princeton, New Jersey 08543-4000

The protein WrbA had been identified as an *Escherichia coli* stationary-phase protein that copurified and coimmunoprecipitated with the tryptophan repressor. Sequences homologous to WrbA have been reported in several species of yeast and plants. We previously showed that this new family of proteins displays low but structurally significant sequence similarity with flavodoxins and that its members are predicted to share the α/β core of the flavodoxin fold but with a short conserved insertion unique to the new family, which could account for reports that some family members may be dimeric in solution. The general sequence similarity to flavodoxins suggests that the members of the new family might bind FMN, but their wide evolutionary distribution indicates that, unlike the flavodoxins, these proteins may be ubiquitous. In this paper, we report the purification and biochemical characterization of WrbA, demonstrating that the protein binds FMN specifically and is a multimer in solution. The FMN binding constant is weaker than for many flavodoxins, being ~2 μM at 25 °C in 0.1 mM sodium phosphate, pH 7.2. The protein participates in a dimer-tetramer equilibrium over a wide range of solution conditions, with a midpoint at approximately 1.4 μM. One FMN binds per monomer and has no apparent effect on the multimerization equilibrium. WrbA has no effect on the affinity or mode of DNA binding by the tryptophan repressor; thus, its physiological role remains unclear. Although many proteins with flavodoxin-like domains are known to be multimers, WrbA is apparently the first characterized case in which multimerization is associated directly with the flavodoxin-like domain itself.

WrbA was first identified by Somerville and co-workers (1) as a protein that copurified and coimmunoprecipitated with the tryptophan (Trp) repressor, TrpR. By band-shift assay, those workers concluded that WrbA influences the binding of TrpR to its operator sequence and that WrbA alone does not bind to that DNA. On this evidence, the protein was named tryptophan (*W*)-*r*epressor *b*inding protein *A*. Sequence analysis and homology-based structural modeling (2) suggested that WrbA was very likely to share the α/β twisted open-sheet fold characteristic of flavodoxins. Comparisons with flavodoxins and with the protein sequence data base (3) identified WrbA as the founding member of a new class of flavodoxin-like proteins containing a well conserved insertion of 24 residues following predicted strand β4. Two other *Escherichia coli* proteins, MioC and the hypothetical protein YihB, are members of the new family but are more closely related to flavodoxins than to other family members, and both lack an insertion in this region. This insertion is itself predicted to form an additional α/β segment and is a strong candidate to be the structural element responsible for experimental reports that WrbA (Ref. 1 and this work) and its homolog in yeast, Ycp4 (4), are dimeric in solution. The modeling results also suggested that the protein presents an active site crevice that could be suitable for flavin binding but with some notable differences from typical flavodoxins, making FMN binding a weak prediction and implying that experimental characterization of ligand binding by WrbA might reveal interesting features. These intriguing leads, coupled with the possibility that this protein might influence a thoroughly studied metabolic regulon, motivated the present biochemical characterization of WrbA.

MATERIALS AND METHODS

Strains—E. coli JM101 (Δ*lac pro supE thi*/*F′traD36 proAB*$^+$ *lacI*^{q}*ZΔM15*) was obtained from Amersham Pharmacia Biotech. The expression strain *E. coli* CY15071(λ *DE3*) (Δ*trpRthr tnaA2 lacI*^{q} λ*DE3*) was constructed (5) by lysogenizing CY15071 (6) with bacteriophage λ (DE3) obtained from Novagen, Inc., according to the manufacturer's protocol.

Cloning—Genomic DNA was prepared from JM101 with the QIAamp tissue kit (Qiagen), following the manufacturer's protocol for bacterial growth. 1 μg of DNA was used as template for 25 cycles of polymerase chain reaction amplification. The sequences of the oligonucleotides used as primers were as follows: 5′ CACACAT**ATG**GCTAAAGTTCTGGT 3′ (upstream of WrbA gene) and 5′ CACAGGATCC**TTA**GCCGTTAAGTTTAAC 3′ (downstream of WrbA gene). Start and stop codons are indicated in bold. Added restriction sites for cloning are underlined (*Nde*I upstream, *Bam*HI downstream). The 596-base pair *Nde*I-*Bam*HI fragment resulting from polymerase chain reaction amplification was cloned into the corresponding sites of pET3a (New England Biolabs), resulting in plasmid pKGWa. The DNA sequence was determined with the chain-terminator method (7). One difference was found from the published sequence (1): bases 711 and 712 of GenEMBL M99166 are given as CG, whereas we read GC. This change also implies a change from Ala to Gly at residue 141 of WrbA protein. Such an alteration is not likely to be the result of polymerase chain reaction amplification, and other members of the family have Gly at that position in the sequence, so it seems likely that the sequence in the data base should reflect this correction.

Protein Analysis—For preparation of total protein extracts, cells were collected, washed with water, lysed by resuspension in the electrophoresis loading buffer (8), boiled for 5 min, and microfuged at 14,000 rpm. The soluble material was used for electrophoresis. Discon-

* This work was supported by National Institutes of Health Grant GM-43558 (to J. C.). The costs of publication of this article were defrayed in part by the payment of page charges. This article must therefore be hereby marked "*advertisement*" in accordance with 18 U.S.C. Section 1734 solely to indicate this fact.

‡ Present address: Institute of Chemistry, Johannes Kepler University, Altenberger Strasse 69, A-4040 Linz, Austria.

¶ Present address: Dept. of Biochemistry, Merck Research Laboratories, Rahway, NJ 07065.

‖ Present address: Biology Dept., Haverford College, Haverford, PA 19041.

** Present address: Yale University Medical School, New Haven, CT 06510.

‡‡ To whom correspondence should be addressed.

tinuous SDS-polyacrylamide gel electrophoresis was performed according to Laemmli (8) in a Bio-Rad minigel apparatus at 12% acrylamide concentration. After electrophoresis, gels were either stained with Coomassie R (1 g/liter in 50% methanol, 10% acetic acid) or blotted to polyvinylidene difluoride membranes in 10 mM CHAPS,[1] pH 11, 10% methanol for sequencing. N-terminal sequencing by Edman degradation and amino acid analysis of proteins were performed by the staff of the Princeton University Molecular Biology Department sequencing facility using standard methods.

Protein Purification—Cells were collected from 1.5 liters of overnight culture grown in LB containing 100 μg/ml ampicillin, resuspended in 40 ml of buffer P (20 mM sodium phosphate, pH 7.2) containing 1 mM phenylmethylsulfonyl fluoride, and broken by one cycle of French press. All subsequent steps were performed at 4 °C. After centrifugation at 30,000 × *g* for 30 min, the sample was applied to a 100-ml DEAE-cellulose (Sigma) column prepared according to the manufacturer's protocol and equilibrated in buffer P. The column was washed with 200 ml of buffer P and developed with a 300-ml linear gradient of NaCl from 0 to 1 M in buffer P with a flux of 2 ml/min. The pool of fractions containing WrbA was dialyzed against buffer P and loaded onto a 25-ml Affi-Gel Blue (Bio-Rad) affinity column prepared according to the manufacturer's protocol and equilibrated in buffer P. The column was washed with 100 ml of buffer P and developed with a 300-ml linear gradient of NaCl from 0 to 1 M in buffer P with a flux of 1 ml/min. The pool of fractions containing WrbA was dialyzed against buffer P and brought to 50% saturation of ammonium sulfate (final 314 g/liter). After 1 h of incubation, the sample was centrifuged at 30,000 × *g* for 30 min, and the supernatant was dialyzed against buffer P and concentrated in Centriprep 10 concentrators (Amicon).

Flavin Analysis—One volume of methanol was added to an aliquot of the dialyzed DEAE-fraction pool and mixed, and the sample was centrifuged at 13,000 × *g* to remove precipitated proteins. The supernatant was concentrated 2-fold by evaporation, additional methanol was added to 20%, and an aliquot was loaded onto a PepRPC HR 5/5 fast protein liquid chromatography reverse-phase column (Amersham Pharmacia Biotech) running in 20 mM sodium phosphate buffer, pH 6, 20% methanol. A standard solution of 10 μM each FMN (Sigma), FAD (Sigma), and riboflavin (Aldrich) was prepared in buffer P containing 50% methanol. Samples were loaded using a 100-μl loop for injection. Flavin concentrations were determined using their known extinction coefficients (9).

Size-exclusion Chromatography—Samples of pure WrbA were loaded onto a prepacked Superdex 75 column (Pharmacia) running at room temperature (22 °C) in buffer P. The column was calibrated with molecular weight standards (Sigma or Bio-Rad unless noted), horse heart cytochrome *c* (12,400 Da), carbonic anhydrase (29,000 Da), ovalbumin (45,000 Da), and blue dextran (void volume). The buffer for TSK column separation was 100 mM potassium phosphate, pH 7.0, 100 mM KCl, and standards were aldolase, gamma globulin (both 158,000 Da, Pharmacia), ovalbumin, and myoglobin (17,000 Da).

Analytical Ultracentrifugation—Sedimentation equilibrium experiments were carried out in a buffer of 50 mM Tris-HCl, pH 7.9, 100 mM NaCl, 10 mM $MgCl_2$ at 4 °C in a Beckman model XLA analytical ultracentrifuge using an AN-60-Ti rotor (10). Data were collected using standard 12-mm path length, six-channel, charcoal-filled Epon cells with quartz windows. Continuous radial scanning at wavelengths between 238 and 285 nm was used for 5 to 10 μM samples. The cells were scanned every 0.001 cm at each of several rotor speeds, and 10 scans were averaged at each speed. The default value of 1.0017 g/ml was used without correction for the solvent density. The partial specific volume of WrbA was 0.735 ml/g as calculated from the weight-average partial specific volumes of the individual amino acids (11).

Circular Dichroism—Far-UV CD spectra were acquired in buffer P at 25 °C on an Aviv model 62DS spectropolarimeter using a 0.1- or 1.0-cm path length quartz cell except for samples at submicromolar concentrations, where a 10-cm path length cylindrical cell was used.

FMN Binding—Fluorometry data were acquired using a SPEX 1680 Double Beam Spectrometer and analyzed using the SPEX dm3000 program (1 μM data) or a Perkin Elmer LS 50 luminescence spectrometer and analyzed using the Perkin Elmer FL program (5 μM data). 1-cm path length cuvettes with 300-μl volumes were used for 1 μM titrations, and cuvettes with 500-μl volumes were used for 5 μM titrations. Samples were equilibrated at room temperature for at least 1 h after mixing prior to measurements. Emission spectra were generated using an excitation wavelength of 459 nm. The decrease in the concentration of free FMN was determined from the fluorescence emission integrated over the range 480 to 680 nm. Determination of dissociation constants and binding stoichiometry was done by standard nonlinear least squares fitting procedures using MLAB (12); (Civilised Software, Inc., Bethesda, MD), with posttransition baseline values determined from the fit as indicated in Fig. 3*B*.

Gel Mobility Shift Assays—Gel mobility shift titration experiments were performed as described by Yang *et al.* (1) with some modifications. An ^{35}S end-labeled *Bam*HI-*Eco*RI 100-base pair DNA fragment containing the *trp EDCBA* promoter/operator sequence of *Serratia marcescens* was prepared as described previously (13) from plasmid pRK9 (14) and purified from a 6% acrylamide gel by the crush-and-soak method of Sambrook *et al.* (15). DNA concentration was estimated visually from ethidium bromide-stained gels. Approximately 0.03 nM DNA fragment was incubated with different amounts of protein(s) in a final volume of 20 μl of 20 mM Tris acetate, pH 7.9, 10 mM magnesium acetate, 50 mM potassium acetate, 1 mM dithiothreitol, 10% glycerol, 50 ng/μl poly(dI-dC)/poly(dI-dC) for 20 min at 37 °C. The samples were loaded onto a pre-electrophoresed 10% polyacrylamide gel running at 100 V at room temperature. The gel and running buffer contained 10 mM Tris-HCl, pH 7, 1 mM EDTA, 0.5 mM L-tryptophan. Electrophoresis was performed at constant voltage for 2.5 h with buffer recirculation.

RESULTS

Expression and Purification of WrbA—The WrbA gene was amplified from *E. coli* genomic DNA on the basis of the published sequence (1) using the polymerase chain reaction and cloned in plasmid pET3a for expression under the control of T7 RNA polymerase (16) in host strain CY15071(λDE3) (5), which is deleted in its chromosomal copy of the gene for TrpR (6) to avoid TrpR contamination in protein purification. High level expression of a polypeptide with the expected relative molecular mass of ~21,000 Da was observed after overnight growth in rich medium (Fig. 1*A*, *lane 2*). As already reported by Somerville's group (1), we also see that addition of 1 mM isopropylthiogalactoside does not increase expression levels, presumably because of the leakiness of the T7 expression system. Identity of the overproduced protein was confirmed by 10 cycles of N-terminal sequencing after blotting of a sample like that in *lane 2* of Fig. 1*A*. As already reported (1), the mature protein starts with Ala following the initial Met.

The purification strategy was based on published methods for flavodoxins (17) in an attempt to retain the predicted flavin cofactor. The dark gray color of the harvested cell paste is typical of cells overexpressing flavoproteins (18). A French press extract of the cell paste was loaded onto a DEAE-cellulose column developed with a linear gradient of NaCl. A deep yellow peak eluted at around 300 mM salt. The pool of yellow fractions had an absorption spectrum typical of flavoproteins (Fig. 1*B*) and was found to be enriched in WrbA by SDS-polyacrylamide gel electrophoresis (Fig. 1*A*, *lane 3*). Trial-scale experiments showed that WrbA bound to Affi-Gel Blue, as well as to Matrex Red A, resins, as do several other nucleotide-binding proteins (19), and could be eluted by salt but not by 100 μM FMN or by 10 mM NAD or NADP, but the flavin cofactor was invariably lost upon elution. A preparative Affi-Gel Blue column developed with a linear NaCl gradient yielded WrbA apoprotein at around 300 mM salt (Fig. 1*A*, *lane 4*). Following 50% ammonium sulfate precipitation, the supernatant was found to be essentially pure WrbA apoprotein (Fig. 1*A*, *lane 5*). Typical final yields were ~10 mg per liter of cell culture with final purity of at least 96%. The extinction coefficient of the pure apoprotein at 280 nm was determined by the method of Gill and von Hippel (20) to be 22,831 M^{-1} cm^{-1}.

Identity of Flavin Cofactor—Enriched preparations of WrbA after DEAE-column chromatography were used as the starting material for analysis of flavin content. A sample of the DEAE pool was extracted with 50% methanol and analyzed by reversed-phase column chromatography. The methanol-extract-

[1] The abbreviations used are: CHAPS, 3-[cyclohexylamino]-1-propanesulfonic acid; BSA, bovine serum albumin.

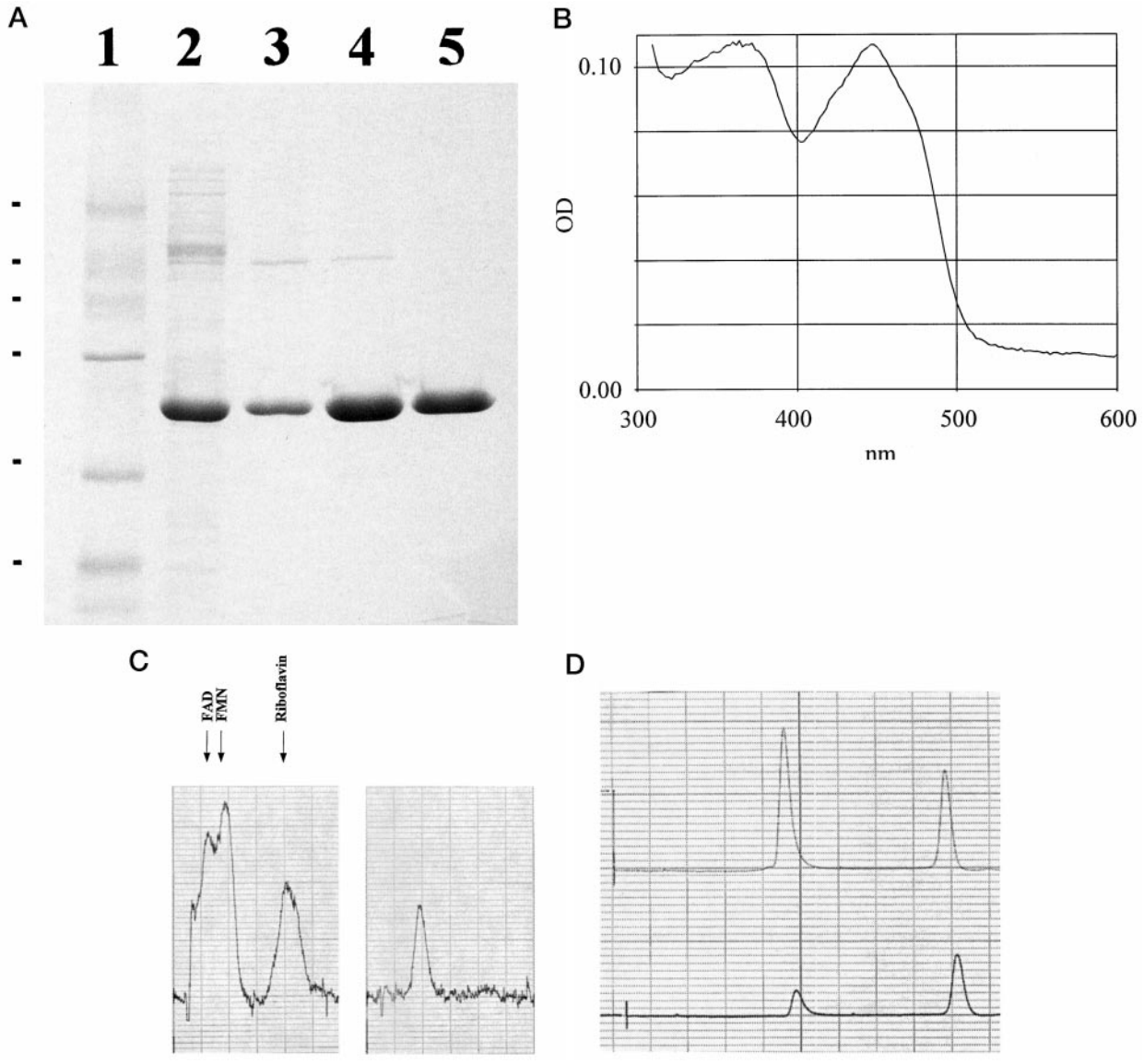

FIG. 1. **Purification of WrbA protein and identification of its cofactor.** *A*, purification of WrbA protein, analyzed by Coomassie Blue-stained SDS-polyacrylamide gel electrophoresis. *Lane 1*, molecular weight markers; *top* to *bottom*: BSA, 66 kDa; ovalbumin, 45 kDa; glyceraldehyde-3-phosphate dehydrogenase, 36 kDa; carbonic anhydrase, 29 kDa; soybean trypsin inhibitor, 20 kDa; α-lactalbumin, 14 kDa. *Lane 2*, crude extract of *E. coli* CY15071(λDE3) cells overexpressing WrbA from clone pKGWa (sample loaded onto DEAE column). *Lane 3*, pool of yellow fractions eluting at ~300 mM NaCl from DEAE column. *Lane 4*, pool of fractions eluting at ~300 mM NaCl from Affi-Gel Blue column. *Lane 5*, supernatant from 50% ammonium sulfate precipitation of Affi-Gel Blue column pool. Approximately 2.5 μg of total protein was loaded in *lane 5*, and the detection limit in the gel is ~0.1 μg; thus, the protein is estimated to be at least 96% pure. *B*, UV-visible absorption spectrum of pooled DEAE-column fractions (equivalent to the sample in *lane 3* in *panel A*). OD, optical density. *C*, cofactor identity, analyzed by reversed-phase column chromatography. Elution profiles detected by absorbance at 450 nm are shown. *Left*, commercial standards FAD, FMN, and riboflavin (10 μM each) from *left* to *right*, respectively. *Right*, methanol-extractable material from the DEAE-column pool. The point of injection is marked by the *vertical line* at the *far left* of each panel. One *horizontal scale mark* corresponds to A_{450} of 0.001; one *vertical scale mark* corresponds to 2.0 ml. The sensitivity settings were dictated by that required for the amount of material in the methanol extract. *D*, resolution of reconstituted WrbA holoprotein and free FMN by size-exclusion chromatography. The elution profiles detected by absorbance at 280 (*upper line*) and 450 nm (*lower line*) are shown for a mixture of 36 μM WrbA apoprotein with 50 μM FMN. The two wavelengths are detected simultaneously but are offset slightly because of the configuration of the recorder pens, as indicated by the point of injection marked by the *vertical line* at the *far left*. One *horizontal scale mark* corresponds to an absorbance of 0.002; one *vertical scale mark* corresponds to 2.0 ml.

able material eluted as a single peak (Fig. 1*C*, *right*) with the same retention time as an FMN standard, which was clearly resolved from riboflavin and FAD (Fig. 1*C*, *left*). The absorbance spectrum of the methanol extract was indistinguishable from that of the FMN standard (not shown). Estimation of extracted FMN and WrbA protein concentrations in the pool, calculated using their respective extinction coefficients, indicated approximately 1 FMN per 10 monomers.

Reconstitution of WrbA Holoprotein—Pure WrbA apoprotein and an excess of commercial FMN were incubated together and resolved by size-exclusion column chromatography (Fig. 1*D*). FMN was identified in the elution profile by its absorbance at 450 nm, where WrbA apoprotein has no absorbance, and was found in two peaks, one with the same retention time as WrbA apoprotein and the other with the retention time of free FMN. At similar concentrations, neither FAD nor riboflavin comigrated with WrbA, nor was the retention time of FMN affected by prior incubation with BSA (data not shown). Thus, WrbA binds FMN specifically and reversibly. Equilibration times as short as 5 min yielded equivalent results, indicating a relatively rapid association reaction. Although the facile loss of the cofactor during purification suggests a rapid dissociation rate,

the very minor tailing in the elution profile of the reconstituted holoprotein indicates that the dissociation rate of FMN is slow on the time scale of this column. The amount of bound FMN changed with FMN or protein concentration and reached a plateau at high FMN concentrations, indicating saturation of available binding sites. Quantitation of free and bound species using the peak areas (data not shown) indicated an average stoichiometry of 0.97 FMN per WrbA monomer at saturation (S.D. 0.08; $n = 6$).

Multimeric State—The elution profiles of both apo- and holoprotein WrbA on the Superdex 75 size-exclusion column used for resolving the reconstituted holoprotein by fast protein liquid chromatography were little changed over a wide range of conditions (flow rate (0.1 or 1.0 ml/min), temperature (~4° or ~22 °C), and addition of 1 M NaCl, 0.1% Triton, or various concentrations of FMN), although the elution time decreased slightly as protein concentration increased over the range 0.1 to 10 μM, suggesting a rapid multimeric equilibrium. The protein elutes too close to the molecular weight cutoff of approximately 70 kDa on this column for accurate determination of its apparent molecular weight. Analysis on a TSK-G3000SWxl high pressure liquid chromatography size-exclusion column (molecular mass cutoff ~150,000 Da) gave an apparent molecular mass of ~62,000 Da at an initial WrbA concentration of 8 μM (data not shown), confirming the multimeric state of the protein on a second resin type. The protein-concentration dependence of the gel filtration results is indicative of a system involved in rapid subunit equilibria.

The quaternary structure of WrbA was therefore further examined by analytical ultracentrifugation at several concentrations (Fig. 2A and Table I), which confirmed the presence of a multimeric equilibrium. Simultaneous fitting of the sedimentation equilibrium data collected at different centrifugation speeds was used to derive an average apparent molecular mass (M_r) for each sample, assuming the presence of only a single species. At loading concentrations of 5–10 μM WrbA (monomer), this analysis resulted in an average apparent molecular mass of approximately 74 kDa, implying an association of 3.6 monomers. This result rules out the monomer as the dominant species of WrbA at micromolar protein concentrations and provides support for the existence of a dynamic equilibrium involving at least one higher order species in this range of initial protein concentrations.

To evaluate different possible scenarios for multimerization of WrbA, the square root of variance (Table I) and randomness of residuals, two measures of the goodness of fit, were compared for fitting of the data to various models of subunit equilibrium. Because of literature reports that members of the WrbA family may be dimeric in solution (1, 4), we included both monomer–*n*-mer and dimer–*n*-mer models in our analysis. Several models could be excluded because of failure to converge on a solution (monomer–*n*-mer, where $n < 4$) or because of poor fit, nonrandomness of residuals, and/or increased square root of variance (all single species models, and all monomer–*n*-mer or dimer–*n*-mer models where $n > 4$). Two models, monomer-tetramer and dimer-tetramer, gave nearly equally good fits as judged by square root of variance and the randomness of residuals. The sedimentation equilibrium data alone cannot distinguish between these two models, as the fits are essentially equivalent. As justified by the experiments reported in the following paragraphs, the fit shown in Fig. 2*A* is that for the dimer-tetramer model.

The apparent dissociation constants describing these two models are 2.6×10^{-17} M^3 for the monomer-tetramer model and 1.4×10^{-6} M for the dimer-tetramer model. To directly compare these two values, we used the relation $(M_T)_{1/2} = 2(1/4\ K_d)^{1/3}$

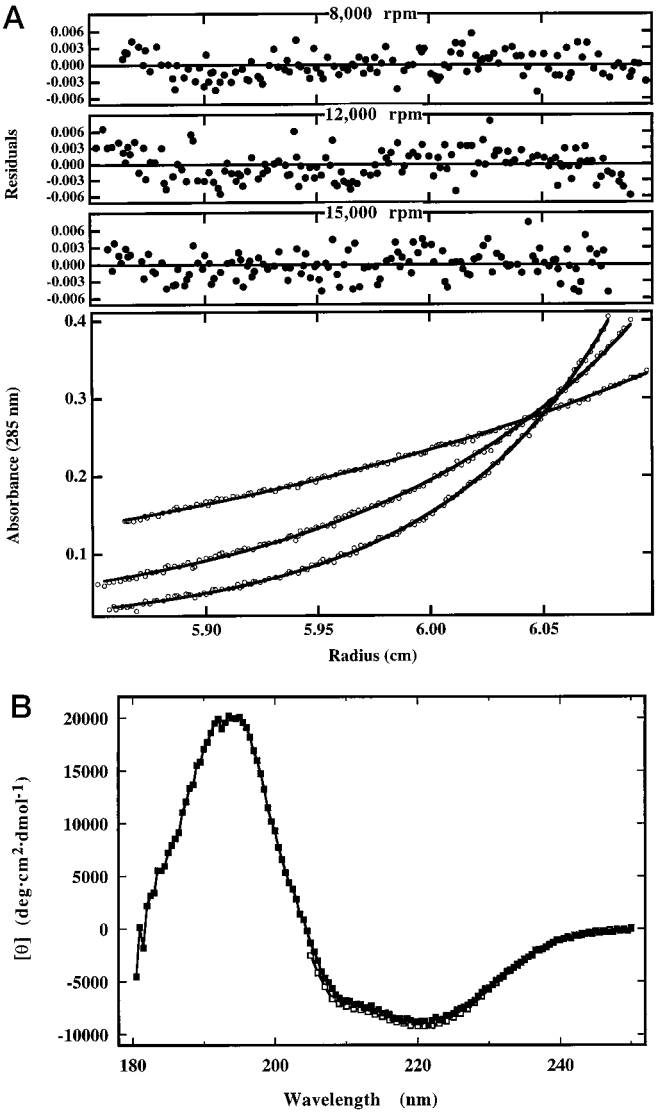

FIG. 2. **Multimeric state of WrbA apoprotein.** *A*, equilibrium sedimentation ultracentrifugation. *Bottom*, radial distribution of WrbA concentration detected by absorbance at 285 nm at three rotor speeds (8, 12, and 15 krpm, respectively, from *top* to *bottom* at *lower left*) using a loading concentration of 10 μM WrbA at 4 °C in 50 mM Tris-HCl, pH 7.9, 100 mM NaCl, 10 mM $MgCl_2$. The *solid lines* show a global fit of the three data sets to a dimer-tetramer model with $K_d = 1.4$ μM. *Top*, residuals for fit of data at each respective speed to dimer-tetramer model. *B*, far-UV CD spectrum of WrbA apoprotein in buffer P. Mean residue ellipticity (y axis) is shown for 5.76 μM protein (*filled squares*) and for 0.36 μM protein (*open squares*). The spectra were normalized to zero at 250 nm and corrected for the buffer blank. In the 10-cm cell used for the lower concentration sample, absorption interference from the buffer increases the scatter in the data to unacceptable levels at wavelengths lower than about 205 nm.

introduced by Bujalowski and Lohman (21) to calculate $(M_T)_{1/2}$, the concentration of total protein (as monomer) at the transition midpoint for the monomer-tetramer model. The value of $(m_T)_{1/2}$, in this case 3.7×10^{-6} m, can be directly compared with the K_d for the dimer-tetramer model. Thus by either model, the midpoint of the oligomerization transition occurs in the micromolar concentration range.

To determine which of the two models correctly describes the WrbA system, each dissociation constant for tetramer formation was used to calculate the predicted species distributions for monomer, dimer, and tetramer as a function of protein concentration according to each model. The monomer-tetramer model predicts essentially only monomer at protein concentra-

TABLE I
Analysis of sedimentation equilibrium data

Data were collected at 4 °C with detection at 238 nm for 5 μM, 280 nm for 9 μM, and 285 nm for 10 μM samples and analyzed using the HID program from the Analytical Ultracentrifugation Facility at the University of Connecticut. Analysis was carried out using global fits to data acquired at 6,000, 10,000, and 15,000 rpm for 5 μM protein, at 10,000, 15,000, and 20,000 rpm for 9 μM protein, and at 8,000, 12,000, and 15,000 rpm for 10 μM protein.

[WrbA][c]	M_r[d]	SRV[a]						$1nK_a$[b]	
		SS[e]	1–3[f]	1–4[f]	1–5[f]	2–4[f]	2–6[f]	1–4	2–4
μM									
5.0	74,144 ± 5,300	4.38	NS[g]	4.35	4.45	4.35	4.44	39.0 ± 0.8	14.0 ± 0.4
9.0	73,288 ± 1,900	2.93	NS[g]	3.15	5.29	2.94	4.90	37.9 ± 0.7	13.2 ± 0.3
10.0	74,360 ± 3,500	2.58	NS[g]	2.48	2.59	2.51	2.58	37.7 ± 0.7	13.3 ± 0.4

[a] SRV, square root of variance ($\times 10^3$).
[b] $1nK_a$, natural log of the association constant; average values: 1–4, 38.2; 2–4, 13.5.
[c] Concentration of protein loaded.
[d] M_r, the apparent molecular mass in Daltons, determined from single-species analysis.
[e] SS, single species.
[f] Monomer–*n*-mer or dimer–*n*-mer equilibria of increasing order.
[g] NS, no solution.

tions between 0.1 and 1 μM, whereas the dimer-tetramer model predicts a significant fraction of dimer in this concentration range. These predictions were then evaluated experimentally by determining the average apparent molecular weight at various protein concentrations using size-exclusion chromatography (data not shown), taking advantage of the observation that the apparent molecular weight on gel filtration depended on loading concentration. The apparent molecular mass determined by size-exclusion chromatography on high pressure liquid chromatography at a loading concentration of 0.1 μM WrbA is approximately 48 kDa, in reasonable agreement with the average molecular mass expected (45 kDa) for a rapid dimer-tetramer equilibrium with a K_d of 1.4 μM, and inconsistent with the prediction of the monomer-tetramer model (21 kDa).

The apparent molecular weights obtained by gel filtration at low protein concentrations cannot be explained by the presence of an unfolded monomer with a large hydrodynamic radius because CD analysis of WrbA apoprotein in the submicromolar concentration range, measured using a 10-cm path length cell, shows spectral features identical to those observed at higher protein concentrations (Fig. 2*B*). Furthermore, this is the far-UV CD spectrum expected for a well folded, mixed α/β protein. The spectrum is unaffected by addition of FMN. Thus, the combined analysis using ultracentrifugation, gel filtration, and circular dichroism allows a clear distinction between the two models for multimerization and indicates that WrbA participates in a rapid dimer-tetramer equilibrium over a range of protein concentrations and solution conditions, with a midpoint concentration of 1.4 μM dimer at pH 7.9 in 50 mM Tris-HCl, 0.1 M NaCl, 10 mM $MgCl_2$, 4 °C.

FMN Binding—Quantitative analysis of FMN binding was carried out by fluorescence titration. The high quantum yield of fluorescence emission by FMN is greatly reduced upon binding of WrbA, as is the case for many flavodoxins (18). Preliminary range-finding titrations using fixed FMN concentrations and increasing concentrations of WrbA indicated a binding constant in the low micromolar range. Thus, complete titrations were carried out at 1 to 5 μM FMN (Fig. 3). At 1 μM FMN, the titration data (Fig. 3*A*, *filled squares*) are well fit by a theoretical binding isotherm calculated for 1:1 binding (one FMN per WrbA monomer, *solid line*) with an apparent binding constant (K_d) of 1.98 ± 0.25 μM, although nearly equally good fit is obtained with the theoretical isotherm calculated for noncooperative 1:2 binding with a binding constant of 0.67 ± 0.12 μM (*dashed line*). Titrations at concentrations at or above the binding constant permit more accurate determination of stoichiometry but at the expense of the accuracy of the determined binding constant (22). As shown in Fig. 3*B*, titration data obtained at 5 μM FMN are much better fit by the 1:1 binding isotherm (*solid line*) than by the 1:2 isotherm (*dashed line*), in agreement with the 1:1 stoichiometry determined by gel filtration. Taken together, the results indicate 1:1 binding and an affinity (K_d) of approximately 2 μM at room temperature (~25 °C) in 10 mM sodium phosphate, pH 7.2.

DNA Binding Analysis—Somerville's group (1) found that WrbA influenced the interaction between TrpR and the trpEDCBA operator at high concentrations of TrpR. To determine if WrbA affects the affinity or mode of binding of TrpR to its operator, the effect of WrbA was examined in a TrpR titration experiment at concentrations near the TrpR dissociation constant of ~0.3 nM (Fig. 4). Fig. 4*A* displays the titration of a 100-base pair *trp* EDCBA operator DNA fragment from *S. marcescens* with TrpR holoprotein, showing the expected apparent binding constant as judged by the depletion of half the free DNA at 0.3 to 0.75 nM TrpR and the formation of both 1:1 and 2:1 TrpR:DNA complexes (23). Similar to the previously reported results (1), the presence of WrbA apoprotein at 5 μM (monomer) correlated with a modest increase in the apparent affinity of TrpR for this operator (Fig. 4*B*). However, the effect of WrbA was independent of the addition of FMN (Fig. 4*C*), and the same effect was observed with equivalent concentrations of BSA (Fig. 4*D*); BSA may act through a volume-exclusion mechanism (24). The same effect of added WrbA or BSA was observed with incubation at either 0 or 37 °C. Addition of WrbA or BSA has no effect on the mode of TrpR binding, as judged from the relative amounts of 1:1 and 2:1 TrpR:DNA complexes (*middle* and *upper bands*, respectively). Thus, WrbA does not specifically influence the affinity or mode of binding of TrpR to its operator. When the experiment was carried out at micromolar concentrations of both TrpR and WrbA (not shown), a supershifted band similar to that seen previously (1) was detected above the 2:1 TrpR:DNA complex; the supershifted band is unaffected by the presence of FMN and was also observed in control experiments using BSA. As already reported by Somerville's group, apo-WrbA did not bind to the operator DNA (1), nor did holo-WrbA (data not shown).

DISCUSSION

The predicted FMN binding ability of WrbA was first verified during purification of the protein from an *E. coli* strain engineered to overexpress the protein under the control of bacteriophage T7 RNA polymerase. The FMN cofactor was readily lost during purification, suggesting significantly weaker binding than that found for typical flavodoxins (18, 25). Ratios of about 0.1 FMN per WrbA monomer were observed in the first steps of purification, indicating that FMN biosynthesis may be induced

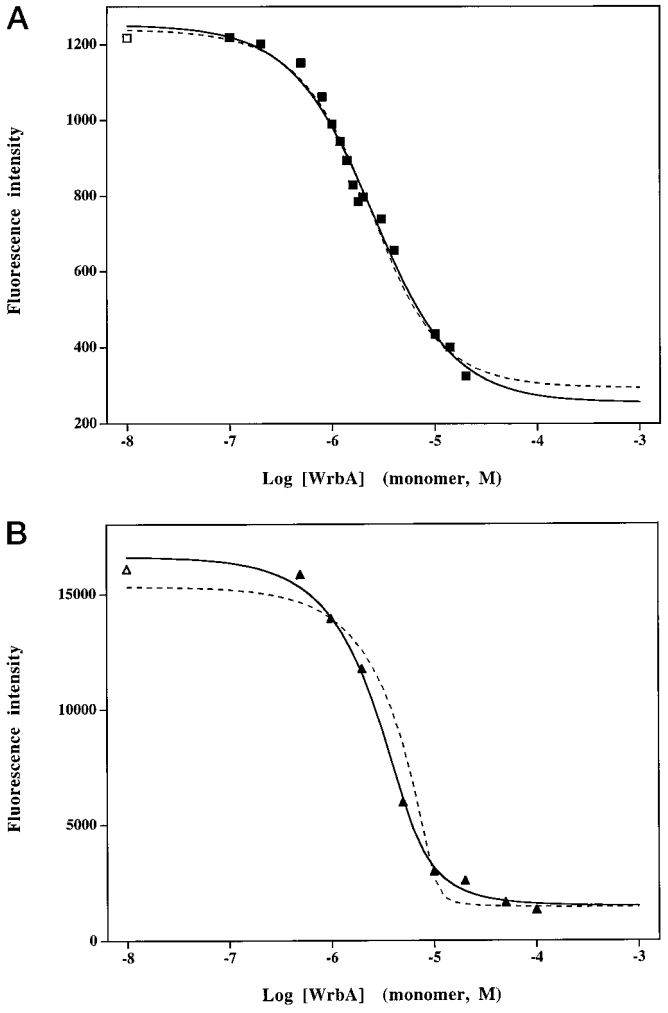

FIG. 3. **FMN binding by WrbA, analyzed by fluorescence titration.** A constant concentration of FMN was titrated with WrbA and monitored by the quenching of FMN fluorescence. Fluorescence intensity (arbitrary units; y axis) is plotted as a function of WrbA concentration (log units; x axis). *Solid curves* are calculated for 1:1 binding stoichiometry and *dashed curves* for stoichiometry of one FMN per WrbA dimer (1:2 stoichiometry), with best-fit apparent binding constant (K_d) given. *Open symbols* at *left* of each panel are experimental values obtained at zero WrbA concentration, for which a log value is undefined, arbitrarily shown at the lowest protein concentration displayed on the log scale. *A*, *squares* indicate data collected using 1 μM FMN; *solid line* indicates K_d 1.98 $\pm$ 0.25 μM; *dashed line* indicates K_d 0.67 $\pm$ 0.12 μM (dimer). Both fits used a final baseline value of 340 $\pm$ 60. *B*, *triangles* indicate data collected using 5 μM FMN; *solid line* indicates K_d 0.68 $\pm$ 0.16 μM; *dashed line* indicates K_d 0.04 $\pm$ 1.1 μM (dimer). Both fits used a final baseline value of 1500 $\pm$ 300.

upon overexpression of WrbA and therefore suggesting that FMN is likely to be the physiological cofactor. FMN could be rebound to the apoprotein in 1:1 stoichiometry at high concentrations of protein and FMN. Weak FMN binding with 1:1 stoichiometry was confirmed by fluorescence titration, which yielded a dissociation constant of approximately 2 μM at room temperature in 10 mM sodium phosphate, pH 7.2. FMN was bound specifically in preference to FAD or riboflavin, strengthening the suggestion that, despite its relatively weak affinity, FMN is the likely physiological cofactor for WrbA. Thus, the prediction of weak but specific FMN binding, based on a structural homology model of WrbA (2), is experimentally confirmed.

The combined results of equilibrium analytical ultracentrifugation and size-exclusion chromatography indicate that the pure apoprotein participates in a rapid dimer-tetramer equilibrium over a wide range of solution conditions, with a mid-

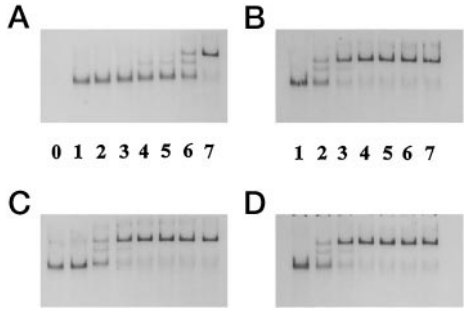

FIG. 4. **Effect of WrbA on TrpR-DNA binding affinity, analyzed by gel shift assay.** The panels show identical titrations with TrpR holoprotein alone (*A*) or in the presence of additional proteins: WrbA apoprotein at 0.1 mg/ml (5 μM monomer) in *B*, WrbA holoprotein (5 μM each of apoprotein monomer and FMN) in *C*, and BSA at 0.1 mg/ml in *D*. In each panel, *lane 1* contains no added TrpR, and *lanes 2–7* contain TrpR at final concentrations of 0.03, 0.075, 0.15, 0.3, 0.75, and 1.5 nM, respectively, whereas *lane 0* (*panel C* only) contains no added TrpR and no other added protein. Sample and running conditions are described under "Materials and Methods."

point at 1.4 μM dimer at 4 °C in 50 mM Tris-HCl, pH 7.9, 100 mM NaCl, 10 mM $MgCl_2$. Although the apparent dissociation constant for the dimer-tetramer system is similar to the K_d for FMN binding, the ligand-binding and multimerization equilibria are evidently not strongly coupled, as FMN binding has no effect on the apparent molecular weight of the protein according to the results of size-exclusion chromatography.

Experiments are under way to determine the redox potentials of FMN bound to WrbA. However, the weak binding of the flavin cofactor and the dynamic equilibrium between dimers and tetramers have complicated measurements of the redox potential. These unique features, which distinguish WrbA from typical flavodoxins, may confer unusual redox potentials as well. When the values of WrbA redox potentials are established, they may limit the range of potential redox partners of WrbA and thereby help in understanding its physiological role.

Gel mobility shift assays demonstrate that WrbA has no specific effect on the affinity of binding of TrpR to its operator DNA target. Because the operator used for these experiments can bind as many as three TrpR dimers sequentially in single and tandem binding modes (23), we can also conclude from the mobility shift results that the presence of WrbA has no effect on the binding mode. Although many connections are possible between WrbA and tryptophan metabolism, none stands out as obvious, and neither we nor Somerville's group detected any specific effects in growth experiments on various strains of *E. coli* with or without a functional TrpR protein (Ref. 1 and data not shown). As well, extensive footprinting analysis *in vivo* at various TrpR concentrations using high resolution chemical probes detected no evidence of proteins other than TrpR and RNA polymerase in the regulatory regions of several natural *trp* operators (23). Although the results do not rule out a physiological connection between TrpR and WrbA, it seems possible that the association observed by Somerville and co-workers may have a structural, rather than functional, basis.

The demonstration that WrbA forms multimers has interesting structural and evolutionary implications. Indeed, the structural model (2, 3) suggests strongly that WrbA does not display the typical modular organization of other multimeric flavodoxin-like proteins characterized to date, in which the monomeric flavodoxin-like domain is fused to a multimerization domain (Ref. 26 and references therein). WrbA instead apparently developed its multimerization function by sequence divergence within the fold of the flavodoxin-like domain. According to our alignment (2, 3), two major regions are highly conserved within the WrbA family and are therefore good can-

didates to be multimerization elements: the 24-residue insertion and the C-terminal region. Investigation of the WrbA structure might therefore reveal a minimalistic structural unit for the multimerization of this family of proteins. An analogous case might be presented by NADPH-sulfite reductase of *E. coli*. Its isolated flavodoxin-like domain has been reported to form multimers and to bind FMN independently of the larger, FAD binding domain (27). The sequence of the flavodoxin domain aligns without insertions on the sequences of monomeric flavodoxins (26). However, quantitative characterization of the multimerization and FMN binding properties of the isolated domain have not been reported as yet, so its similarity to WrbA cannot be evaluated at present. Both the biochemical properties reported here and the previously reported sequence analysis set WrbA apart from typical flavodoxin-like proteins, and thus imply that further studies on its physiological role may be of significant interest.

Acknowledgment—We thank Dr. Saw Kyin and staff in the Synthesis/Sequencing Facility, Molecular Biology Department, Princeton University, for careful analysis of protein samples and for useful discussions; Dr. Tom Lavoie, Bristol-Myers Squibb, for use of the TSK column; June Wong Fukayama for careful proofreading of the manuscript; Sabine Böhm for assistance in preparing the figures; and Ingrid Hughes for assistance in preparing the manuscript.

REFERENCES

1. Yang, W., Ni, L., and Somerville, R. L. (1993) *Proc. Natl. Acad. Sci. U. S. A.* **90,** 5796–5800
2. Grandori, R., and Carey, J. (1994) *Protein Sci.* **3,** 2185–2193
3. Grandori, R., and Carey, J. (1994) *Trends Biochem. Sci.* **19,** 72, 107
4. Toda, T., Shimanuki, M., Saka, Y., Yamano, H., Adachi, Y., Shirakawa, M., Kyogoku, Y., and Yangida, M. (1992) *Mol. Cell. Biol.* **12,** 5474–5484
5. Lavoie, T. A. (1996) *Molecular Origin of Specificity and Cooperativity in the trp Repressor System.* Ph. D. dissertation, Princeton University
6. Paluh, J. L., and Yanofsky, C. (1986) *Nucleic Acids Res.* **14,** 7851–7860
7. Sanger, F., Nicklen, S., and Coulson, A. R. (1977) *Proc. Natl. Acad. Sci. U. S. A.* **74,** 5463–5467
8. Laemmli, U. K. (1970) *Nature* **227,** 680–685
9. Whitby, L. G. (1953) *Biochem. J.* **54,** 437–442
10. Giebeler, R. (1992) in *Analytical Ultracentrifugation in Biochemistry and Polymer Science*, S. E. Harding (Rowe, A. G., and Hortons, J. C., eds) pp. 16–25, Royal Society of Chemistry, Cambridge
11. Cohn, E. J., and Edsall, J. T. (1943) in *Proteins, Amino Acids, and Peptides as Ions and Dipolar Ions*. pp. 370–377, Reinhold Publishing, New York
12. Knott, G. D. (1979) *Comput. Programs Biomed.* **10,** 271–280
13. Carey, J. (1988) *Proc. Natl. Acad. Sci. U. S. A.* **85,** 975–979
14. Nichols, B. P., and Yanofsky, C. (1983) *Methods Enzymol.* **101,** 155–164
15. Sambrook, J., Fritsch, E. F., and Maniatis, T. (1989) *Molecular Cloning: A Laboratory Manual*, 2nd ed., Cold Spring Harbor Laboratory Press, Cold Spring Harbor, NY
16. Studier, F. W., Rosenberg, A. H., Dunn, J. J., and Dubendorff, J. W. (1990) *Methods Enzymol.* **185,** 60–89
17. Vervoort, J., Heering, D., Peelen, S, and van Berkel, W. (1994) *Methods Enzymol.* **243,** 188–203
18. Mayhew, S. G., and Ludwig, M. L. (1975) *Enzymes* **12,** 57–118
19. Tollin, G., and Edmondson, D. E. (1980) *Methods Enzymol.* **69,** 392–406
20. Gill, S. C., and von Hippel, P. H. (1989) *Anal. Biochem.* **182,** 319–326
21. Bujalowski, W., and Lohman, T. (1991) *J. Biol. Chem.* **266,** 1616–1626
22. Weber, G. (1994) *Protein Interactions*, pp. 16–18, Chapman and Hall, New York
23. Yang, J., Gunasekera, A., Lavoie, T. A., Jin, L., Lewis, D. E. A., and Carey, J. (1996) *J. Mol. Biol.* **258,** 37–52
24. Benedict, R. C., Fall., L., Gill, S. J., and Hedlund, B. (1981) *Biophys. Chem.* **13,** 245–252
25. Mayhew, S. G., and Tollin, G. (1991) in *Chemistry and Biochemistry of Flavoenzymes* (Müller, F., ed) Vol. 3, pp. 389–426, CRC Press, Boca Raton, FL
26. Ostrowski, J., Barber, M. J., Rueger, D. C., Miller, B. E., Siegel, L. M., and Kredich, N. M. (1989) *J. Biol Chem.* **264,** 15796–15808
27. Eschenbrenner, M., Coves, J., and Fontecave, M. (1995) *FEBS Lett.* **374,** 82–84